C. R. Physique 3 (2002) 987–997

Physique appliquée/*Applied physics*

DOSSIER

DU COMBUSTIBLE NUCLÉAIRE AUX DÉCHETS : RECHERCHES ACTUELLES

FROM NUCLEAR FUELS TO WASTE: CURRENT RESEARCH

Radionuclides retention: from macroscopic to microscopic

Eric Simoni

IPN, bâtiment 100, Université Paris XI, 91406 Orsay, France

Received 7 February 2002; accepted 8 April 2002

Note presented by Édouard Brézin.

Abstract In order to determine the radionuclides' sorption constants on solid natural minerals, both thermodynamic and structural investigations, using spectroscopic techniques, are presented. The natural clays, that could be used as engineering barriers in the nuclear waste geological repository, are rather complex minerals. Therefore, in order to understand how these natural materials retain the radionuclides, it is necessary first to perform these studies on simple substrates such as single crystal, oxides and silicates, and then extrapolate the obtained results on the natural minerals. We examine in this paper the sorption processes of the hexavalent uranium on zircon ($ZrSiO_4$) and the trivalent curium on a natural clay (bentonite). The corresponding sorption curves are simulated using the results obtained with the following spectroscopic techniques: laser induced spectrofluorimetry, X-ray photoelectron spectroscopy (XPS), X-ray absorption spectroscopy (EXAFS), diffuse reflectance infrared Fourier transform (DRIFT). ***To cite this article: E. Simoni, C. R. Physique 3 (2002) 987–997.***

sorption / radionuclides / spectroscopic investigations / molecular scale / surface complexes

Rétention des radionucleides : du macroscopique au microscopique

Résumé Afin d'accéder aux valeurs des constantes thermodynamiques associées aux processus de sorption des radionucléides, toute étude thermodynamique devrait être couplée à une étude structurale de l'interface qui peut être réalisée au moyen de différentes techniques spectroscopiques. Les argiles qu'il est prévu d'utiliser comme barrière ouvragée pour un ouvrage de stockage de déchets radioactifs, constituent une famille de substrats complexes. Pour comprendre comment elles retiennent les radionucléides, il est nécessaire de réaliser cette étude sur des phases unitaires représentatives, afin de tenter d'extrapoler ensuite ces résultats aux solides naturels. Cela a conduit à étudier une gamme de matériaux, allant du substrat le plus simple (monocristal) au solide le plus complexe (bentonite) en passant par des solides synthétiques monophasés comme des oxydes et des silicates. On examine dans cet article les cas de sorption de l'uraniuim hexavalent sur le zircon ($ZrSiO_4$) et du curium trivalent sur une argile naturelle, la bentonite. Les courbes de sorption correspondantes sont simulées en utilisant les résultats structuraux obtenus à

E-mail address: simoni@ipno.in2p3.fr (E. Simoni).

S1631-0705(02)01352-X/FLA

l'aide des techniques spectroscopiques suivantes ; spectrofluorimétrie laser, spectroscopie de photoélectrons X (XPS), spectroscopie d'absorption X (EXAFS) et diffusion infrarouge (DRIFT). ***Pour citer cet article : E. Simoni, C. R. Physique 3 (2002) 987–997.***

sorption / radionucléides / études spectroscopiques / échelle microscopique / complexes de surface

1. Introduction

In order to evaluate the performance of the confinement of an underground geological nuclear waste disposal, it is necessary to model the radionuclides' migration through the different materials of the barrier [1,2]. The radionuclides are those contained in the waste packages: U, Np, Pu, Am and Cm. Important factor of confinement are the sorption onto minerals and the precipitation/solubility of the radionuclides [3–7]. These two processes depend mainly on various geochemical parameters such as pH, redox potential and ionic strength of the aqueous medium, speciation of the radionuclides taking into account the solid precipitates, surface area of the mineral substrates, acidity and density of the sorption sites. Different approaches of sorption processes are usually used: empirical models using a partition factor (Kd), mechanistic models such as macroscopic ion exchange or microscopic surface complexation [8–13]. Using only these models, the experimental data simulations do not, however, give unambiguous results. Indeed, these determinations, without any experimental validation, could lead, for instance, to arbitrary surface complexes. Consequently, the precise determination of the corresponding thermodynamic constants is not an easy task and an accurate understanding of the mechanisms at a microscopic scale is imperative before any modeling. Therefore, it is necessary to relate the expected surface complexes to the structure of the surface coordination complexes. In order to get such detailed information, several spectroscopic techniques have been be used: laser induced spectrofluorimetry (emission spectra, decay time measurements) (LIFS), X-ray photoelectron spectroscopy (XPS), X-ray absorption spectroscopy (EXAFS and XANES), diffuse reflectance infrared Fourier transform (DRIFT) [14–22]. These techniques lead to the knowledge of the nature of the sorption sites, the determination of the species sorbed on the mineral surface, the identification of an inner- versus outer-sphere or a mono- versus poly-dendate complex and the presence of a precipitate on the surface, and allow us to chose the sorption equilibria in order to determine the corresponding sorption constants. These parameters will then be used as the retardation factor in the geochemical migration codes.

If the substrate studied is a clay, the determination of the sorption sites is not easy because of the different groups which are supposed to interact with the radionuclides. Such solid, which is an alumino-silicate, can present two edges groups (=S–Al–OH, =S–Si–OH) and an interlayer site (=X–). Therefore, a comparison between the spectroscopic results obtained on the clay and on the alumina and silica should be very helpful.

In this paper, the solids $ZrSiO_4$, γ–Al_2O_3, SiO_2 and a bentonite will be used as examples in order to demonstrate the usefulness of spectroscopic investigations prior to the retention of data simulation. The cations studied are Eu(III), U(VI) and Cm(III). They play here the role of structural probes.

2. Experimental section

2.1. Surface characterization

The three solids considered here are $ZrSiO_4$, γ–Al_2O_3, SiO_2 (silica gel 60 H). They have been purchased from Merck company. The specific surface area, determined by N_2–BET method, are 2.2, 140, 380 and 30 m^2/g, and the grain sizes are 10, 10, 63, 15 µm, respectively for $ZrSiO_4$, γ–Al_2O_3, SiO_2 and bentonite.

Before any sorption experiment, the surface of the solids equilibrated with the ions in solution, has to be well-characterized. The surface of a solid in an aqueous medium reacts with the water molecule given hydroxyl groups and developing electrical charges, which both depend on the pH and on the ionic

Table 1. Surface characterization of the solids

$$\equiv\text{S–M–OH} + \text{H}^+ \Longleftrightarrow \equiv\text{S–M–OH}_2^+ \qquad \text{Ka1}$$

$$\equiv\text{S–M–OH} \Longleftrightarrow \equiv\text{S–M–O}^- + \text{H}^+ \qquad \text{Ka2}$$

Compounds	Site density (sites/nm^2)	Specific area (m^2/g)	Acidity constants
$ZrSiO_4$	4.0	2.2	$\equiv$S–Zr–O pKa1 = 5.2
			$\equiv$S–Zr–O pKa2 = −7.0
			$\equiv$S–Si–O pKa2 = −8.2
			$pH_{PIE} = 6.0$
γ–Al_2O_3	1.6	140	$\equiv$S–Al–O pKa1 = 7.9
			$\equiv$S–Al–O pKa2 = −9.2
			$pH_{PIE} = 8.6$
SiO_2	0.7	380	$\equiv$S–Si–O pKa2 = −7.6
			$pH_{PIE} = 6.6$
Bentonite	60 meq/100g	30	

strength of the solution [23–26]. The surface hydroxyl groups constitute ionizable functional groups which determine the amphoteric behavior of the substrate. The corresponding acidity constants have been then determined by potentiometric measurements: titrations of a suspension of the solid by adding either HNO_3 or NaOH under nitrogen atmosphere. The pH_{pzc} value which is the pH value at the point of zero charge is given by the mass titration method; in this method, the pH value, measured versus the different amounts of solid in the suspension, reaches the point of zero charge of this solid for an amount of powder tending towards an infinite value [27]. Moreover, the surface site density has been determined by comparing the titration curve for the suspension with the curve for the background electrolyte. The method to determine the acidity constants using the surface complexation theory and the constant capacitance model (CCM) is well-documented in the literature [12,13,28,29]. The results obtained for the solids considered are summarized in Table 1.

2.2. Sorption procedure

The U(VI) stock solutions have been prepared by dissolution of the solid $UO_2(NO_3)_2{\cdot}6H_2O$ in a 0.5 M KNO_3 solution previously acidified with HNO_3 to avoid hydrolysis of U(VI). In order to prepare uranyl aqueous ions in perchlorate medium, the uranyl nitrate solid was dissolved in 1 M $HClO_4$ and the obtained solution air dried. This procedure was repeated four times until all the nitrate ions were removed.

The last obtained solid has been then dissolved in a 0.5 M $NaClO_4$ solution. The U(VI) concentrations were in both cases around $5 \cdot 10^{-3}$ M.

The curium stock solution is $NaClO_4$ solution of Cm^{3+} (^{248}Cm isotope with a half-life of $3.5 \cdot 10^5$ y) with a concentration around $5 \cdot 10^{-5}$ M in curium.

The uranyl and curium concentrations in solution before and after the sorption process have been determined by alpha liquid scintillation using a TRI-CARB spectrometer (Packard).

Sorption experiments have been performed using batch experiments in polypropylene tubes in order to avoid the cation sorption onto the tube walls. An amount of 200 mg of solid in 10 mL of KNO_3 or $NaClO_4$ (0.1 and 0.5 M) solution is shaken for 24 h in order to hydrate the substrate. Then, after centrifugation (3500 rpm for 30 min), about 250 µL is removed from the supernatant and replaced by the same volume

of the cation solution and adjusted to the desired pH value. The suspension is stirred during 24 hours (previous sorption kinetic studies have shown that two hours are enough to reach the sorption equilibrium), and after centrifugation, the equilibrium pH value of the supernatant is measured. The sorption percentage is determined as the difference between the initial and the final cation concentrations in solution.

2.3. Spectroscopic measurements

All the emission spectra were recorded at room temperature with a Jobin-Yvon SPEX 270M monochromator with a 1200 lines/mm grating. The fluorescence is detected in the range 540–660 nm by a CCD camera (Princeton Instruments Inc.) with a time window of 1 ms width. The excitation is provided by a pulsed Nd:YAG pumped OPO system (Panther) with a pulse energy in a range 4–16 mJ. In order to measure the emission decay, the delay time between the camera gating and the excitation pulse is scanned with time interval between 60–100 µs. The obtained time dependence is fitted to multiexponential law.

The XPS data were collected on an ESCA apparatus with a multidetection electron analyser (VSW CL150, Fixed Analyser Transmission mode – *FAT*). Both survey ($FAT = 90$ eV) and narrow scans ($FAT = 22$ eV) have been carried out with an unmonochromatic Mg $K\alpha$ source (energy at 1253.6 eV and half-width of 0.9 eV) operated at 15 kV and 10 mA. The powdered samples were held on a copper plate under a vacuum of 10^{-9} mbar. The binding energy of the C1*s* line (284.6 eV) have been used to correct the charge effects in order to calibrate the collected spectra. The recorded lines were fitted to a Gaussian–Lorentzian peak shape after subtraction of the background (Shirley baseline).

The uranium L_{III}-edge absorption spectra (17 176 eV) were recorded at the ROBL experimental station at the ESRF facility. The energy calibration was determined by measuring the zirconium absorption edge. The monochromatic beam, with an energy resolution of around 2 eV at the U L_{III}-edge, was obtained with a double crystal Si(111) located between two Pt coated mirrors. All powdered sorbed samples were measured at room temperature in fluorescence mode using a four elements Ge detector. For each sample, around five individual scans were necessary due to the very low concentration of the sorbed ions on the substrate. EXAFS data reduction has been carried out according to the standard procedure by using in-house codes [30]. The Fourier transforms were achieved in the k^3-weighting mode using a Kaiser window. The solids $UO_2(H_2PO_4)_2{\cdot}3H_2O$ and $(UO_2)_2(SiO_4){\cdot}2H_2O$ have been used as reference compounds [31]. Moreover, the backscattering phases and amplitudes for Si and Zr atoms retrodiffusion have been extracted from ab-initio calculated EXAFS spectrum (FEFF.02 code) [32,33].

The DRIFT experiments have been carried out on a Brucker IFS55 FTIR apparatus with MCT detector coupled with a diffuse reflectance set up (Harwick Scientific Co.) sparged from the CO_2. The powdered samples are diluted with KBr. The IR spectra (200 scans) are recorded at room temperature in the range 600–4000 cm^{-1} with a resolution at around 4 cm^{-1}.

3. Results

Results for several different systems are presented in order to give examples of the determination of the nature of the sorption sites, the identification and the structural characterization of the sorbed species.

3.1. Nature of the sorption site

In order to define the surface sorption site on the solids, both XPS and LIFS techniques have been used on the following examples.

3.1.1. $UO_2^{2+}/ZrSiO_4$, UO_2^{2+}/ZrO_2

After immersion in aqueous solution, 0.5 M $NaClO_4$, pH 3, 10^{-3} M in UO_2^{2+}, the solid $ZrSiO_4$ presents two different surface hydroxyl groups that could be represented as $\equiv$S–Zr–O and S$\equiv$Si–O, while there is only $\equiv$S–Zr–O site on ZrO_2 surface. Therefore, the U4f7/2 XPS spectra of both systems $UO_2^{2+}/ZrSiO_4$

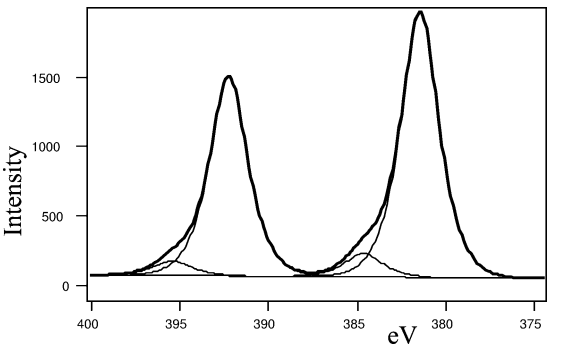

Figure 1. U4f XPS spectrum of UO_2^{2+}/ZrO_2 (dots) and corresponding decomposition (solid line).

and UO_2^{2+}/ZrO_2 have been compared (XPS UO_2^{2+}/ZrO_2 spectrum is presented as example on the Fig. 1). The two spectra present only one component, with the same FWHM of 2.5 eV, at 382.4 eV and 381.5 eV for $ZrSiO_4$ and ZrO_2, respectively. Moreover, the uranium XPS spectrum of the solid $(UO_2)_2SiO_4{\cdot}2H_2O$ [34], not shown here, presents one component as well at 382.2 eV. Consequently, one could assume that the energy value at 381.5 eV corresponds to the binding of uranyl ion on the =S–Zr–O site of ZrO_2 surface, and the one at 382.4 eV is certainly indicative of the link between the uranyl ion and the oxygen atoms of the SiO_4 groups of the $ZrSiO_4$ surface. Furthermore, these results are corroborated by the obtained values of the sorbed uranyl emission decay times. Each system exhibits only one exponential decay with emission lifetime $\tau = 50$ and 23 µs for $UO_2^{2+}/ZrSiO_4$ and UO_2^{2+}/ZrO_2, respectively, which confirms that there are two different environments for the uranyl ions on these two surfaces.

3.1.2. *Eu^{3+}/Al_2O_3; Eu^{3+}/SiO_2, Eu^{3+}/bentonite*

The sorbed trivalent europium XPS binding energies ($3d_{5/2}$) are roughly at the same values (FWHM of 4.5 eV): 1134.5 eV and 1134.8 eV on Al_2O_3 and SiO_2 samples, respectively, when these oxides are equilibrated with a solution 0.1 M $NaClO_4$, $6.2 < \text{pH} < 7.6$, $2 \cdot 10^{-3}$ M in Eu^{3+}. Therefore in this case, it is not possible to distinguish two different environments around the sorbed europium ions. In order to get more precise criteria, LIFS has been used. The europium emission lifetimes τ(Eu) measured are 260 µs for Eu^{3+}/Al_2O_3 ($C(Eu^{3+}) = 2 \cdot 10^{-3}$ M, $NaClO_4$ 0.1 M, $6.2 < \text{pH} < 7.6$), and 160 and 380 µs for Eu^{3+}/SiO_2 ($C(Eu^{3+}) = 2 \cdot 10^{-3}$ M, $NaClO_4$ 0.1 M, $6.2 < \text{pH} < 7.6$). These results indicate that there is actually only one environment for the europium on Al_2O_3, but there are two different ones on the SiO_2 surface.

In the case of an europium solution equilibrated with the bentonite, two different samples, prepared at pH equal at 3.5 and 5.9 ($C(Eu^{3+}) = 2 \cdot 10^{-3}$ M) have been examined. For both samples, the XPS spectra (not shown here) present two components at 1134.7 and 1136.1 eV. Moreover, there is only one component at 1136.1 eV for the XPS spectrum in the case of an europium perchlorate solution ($C(Eu^{3+}) = 2 \cdot 10^{-3}$ M, $\text{ph} = 3.2$, $NaClO_4$ less than $5 \cdot 10^{-2}$ M) equilibrated with the bentonite. The corresponding τ(Eu) values are the following:

– europium solution equilibrated with the bentonite at pH 3.5 : 75, 170 and 260 µs;
– europium solution equilibrated with the bentonite at pH 5.9 : 75, 170, 387 and 260 µs;
– europium perchlorate solution with the bentonite at pH 3.2 : 75 µs.

The comparison of all these results lead to the following conclusions:

The energy at 1136.1 eV and the value $\tau(\text{Eu}) = 75$ µs correspond to an europium ion located between the interlayer space inside the bentonite. This location corresponds to an ion exchange mechanism with the cations of the background electrolyte. According to the Horrocks method which uses a linear relation between the number of coordination water molecules and the emission decay time [35,36], this ion is surrounded by 9 water molecules. The lifetime value $\tau(\text{Eu}) = 260$ µs corresponds to an aluminol site and the values $\tau(\text{Eu}) = 170$ and $\tau(\text{Eu}) = 387$ µs to the silanol site of the bentonite. Therefore, for the europium solution equilibrated with the bentonite prepared at $\text{pH} = 3.5$, the sites which interact are the interlayer site,

the aluminol and one of the two silanol edge sites. For the same sample prepared at pH = 5.9, the second silanol edge site interacts as well. Moreover, since the emission lifetimes of the europium hydroxide and carbonate precipitates are around 220 and 95 µs, respectively, no such precipitates have been found on the bentonite [37].

3.1.3. *Cm^{3+}/Al_2O_3; Cm^{3+}/SiO_2, Cm^{3+}/bentonite*

The same measures as for the Eu systems have been performed on these systems, excepted the XPS investigations due to the very low curium concentration on the solids. Table 2 summarizes all the curium emission decay values measured for these three systems and Fig. 2 shows the curium emission spectra. The Cm^{3+}/Al_2O_3 emission spectrum exhibits only one peak at 604.6 nm, while the Cm^{3+}/SiO_2 emission can be decomposed into two peaks at 607.7 and 616.2 nm. The interpretation of these data is the same as the one proposed for the europium ion. The value $\tau(\mathrm{Cm}) = 85$ µs corresponds to the Cm^{3+} occupying the ion exchange site, $\tau(\mathrm{Cm}) = 170$ µs corresponds the Cm on the aluminol edge site and $\tau(\mathrm{Cm}) = 235$ and $\tau(\mathrm{Cm}) = 730$ µs correspond to Cm on two silanol edge sites on the bentonite. The occupation rate of these sorption sites depends on the pH value of the suspension. For example, at pH = 3.1, the exchange site and the aluminol edge sites interact with the Cm^{3+}, while at pH equal 8.1, only the two silanol edge sites interact with the Cm^3. All these results will be used in the modeling of the curium retention data (see Section 3.4).

Table 2. Curium emission decay values ($\lambda_{\mathrm{excitation}} = 468$ nm)

Compounds	Equilibrium pH	Decay times ±10 (µs)
Cm^{3+}/Al_2O_3 ($NaClO_4$ 0.1 M)	7.1	180
Cm^{3+}/SiO_2 ($NaClO_4$ 0.1 M)	7.0	230/1230
Cm^{3+}/bentonite (solution equilibrated with the clay)	3.1	85/170
	8.1	235/740

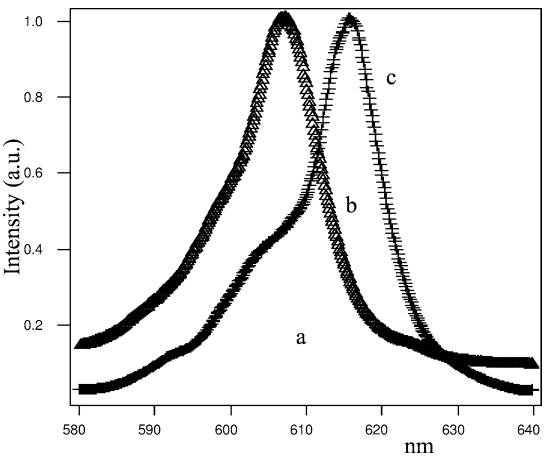

Figure 2. Curium emission spectra ($\lambda_{\mathrm{excitation}} = 468$ nm): (a) Cm^{3+}/Al_2O_3; (b) Cm^{3+}/bentonite; (c) Cm^{3+}/SiO_2.

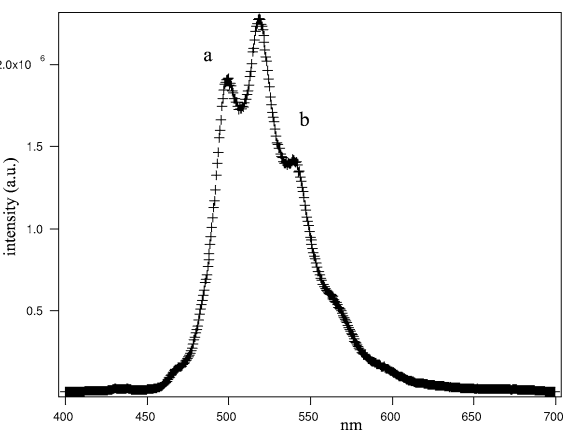

Figure 3. UO_2^{2+}/Al_2O_3 fluorescence spectrum ($\lambda_{\mathrm{excitation}} = 432$ nm): (a) nitrate medium; (b) perchlorate medium.

3.2. Identification of the species sorbed on the surface

The two systems $UO_2^{2+}/ZrSiO_4$ and UO_2^{2+}/Al_2O_3 are given as examples, to demonstrate the use of the spectroscopic technique to identity the species sorbed on the surface in relation to the ion speciation in solution. The effect of the nitrate ions complexation will be examined. We recorded the emission spectra, Fig. 3, and the corresponding decay times of the $UO_2^{2+}/ZrSiO_4$ ($C(U) = 10^{-3}$ M, pH = 3) and UO_2^{2+}/Al_2O_3 ($C(U) = 10^{-4}$ M, pH = 4.2) samples prepared with $NaClO_4$ (0.5 M) and with KNO_3 (0.5 M) as background electrolytes. The uranium speciation diagram (uranium concentration about 10^{-4} M) indicates that uranyl ion (pH < 3.5) is not complexed in perchlorate medium, while in nitrate medium, there is around 80% of UO_2^{2+} and 20% of $UO_2NO_3^+$ in the solution [38]. The lifetime values for $UO_2^{2+}/ZrSiO_4$ sample are $\tau(U) = 50$ and $\tau(U) = 53$ µs in perchlorate and nitrate media, respectively, while it is found for UO_2^{2+}/Al_2O_3 one value $\tau(U) = 55$ µs with $NaClO_4$ salt and two values at 55 and 100 µs with KNO_3 salt. Consequently, the same value in both media for $UO_2^{2+}/ZrSiO_4$ indicates that there is only one species, UO_2^{2+}, on the $ZrSiO_4$ surface, while the two values measured for UO_2^{2+}/Al_2O_3 in nitrate medium indicates clearly that there are two different species, the UO_2^{2+} ion and the nitrate complex $UO_2NO_3^+$ on the Al_2O_3 surface.

In order to confirm the results obtained on the $UO_2^{2+}/ZrSiO_4$ samples, DRIFT experiments have been performed on the solid $ZrSiO_4$ without uranyl ions and on the loaded solid prepared with the nitrate background electrolyte. The vibration spectra, shown in Fig. 4, left, exhibit two main regions at 500–1000 cm^{-1} corresponding to the Zr–O/Si–O elongations and at 1500–4000 cm^{-1} corresponding to the sorbed water molecules. However, any difference between the two samples is observed in the nitrate region 1000–1500 cm^{-1}, which is in agreement with the LIFS results. For comparison, the DRIFT spectra for pure and uranyl loaded ZrO_2 samples, prepared in nitrate medium, are shown on Fig. 4, right. In that case, the bands at around 1000 cm^{-1} and at 1250–1550 cm^{-1} indicate clearly the presence of uranyl nitrate complex on the ZrO_2 surface.

Furthermore, for the $UO_2^{2+}/ZrSiO_4$ sample prepared in a perchlorate medium at pH 5.2, another $\tau(U)$ value has been measured at 20 µs. This value does not correspond to the sorbed UO_2^{2+} but probably to the polynuclear complex $(UO_2)_3(OH)_5^+$, which has already been observed on the titanium surface [39].

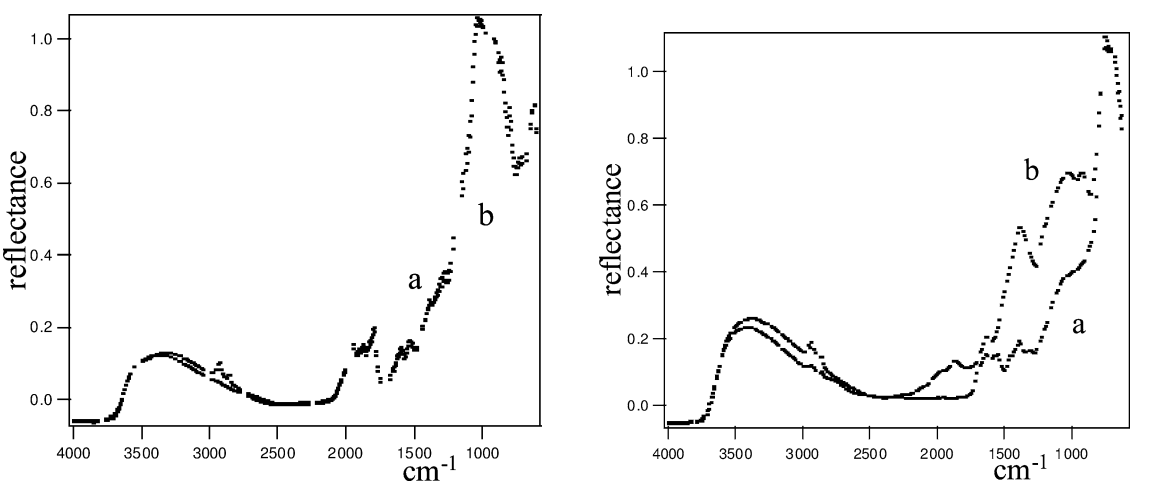

Figure 4. Left: $ZrSiO_4$ DRIFT spectra: (a) pure $ZrSiO_4$; (b) $UO_2^{2+}/ZrSiO_4$. Right: ZrO_2 DRIFT spectra: (a) pure ZrO_2; (b) UO_2^{2+}/ZrO_2.

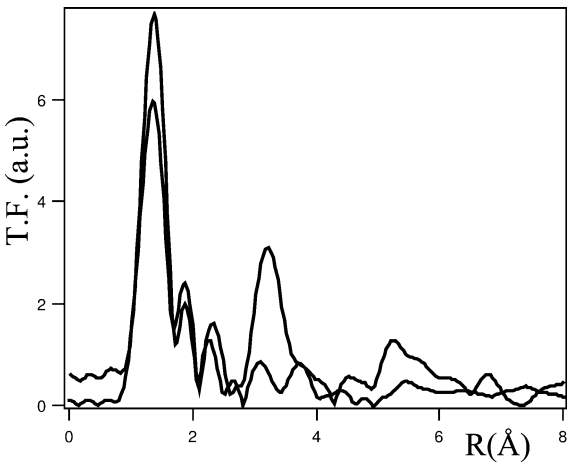

Figure 5. $UO_2^{2+}/ZrSiO_4$ Fourier transforms (straight line pH = 3, dots pH = 5).

Table 3. $UO_2^{2+}/ZrSiO_4$ EXAFS parameters

	pH	N	$R \pm 0.02$ (Å)	σ^2 (Å^2)
U–O_{ax}.	3.0/5.4	2.2	1.81	0.0004
U–O_{eq}.	3.0	3.0	2.36	0.0049
		2.0	2.54	0.0049
	5.4	2.7	2.35	0.0064
		1.8	2.54	0.0064
U–Si	3.0	1.0	2.76	0.0009
	5.4	1.0	2.73	0.0025

3.3. Structural characterization of the sorbed species on the surface

The sample $UO_2^{2+}/ZrSiO_4$ is used, as an example, to show how it is possible to determine the link between the sorbed species and the oxygens of the surface functional groups such as mono- or multi-dentate and outer- or inner-sphere complexes by using uranium L_{III}-edge X-ray absorption spectrum. The XANES region (not shown here) presents the characteristic shape due to the UO_2^{2+} with a white-line energy at 17176 eV and two shoulders that account for multiple scattering along the uranyl rod and for mixing of single and multiple scattering. The Fourier transforms (not phase-shift corrected) of the EXAFS spectra for samples prepared at pH 3 and 5.4, ($C(U) = 10^{-3}$ M) are shown on the Fig. 5. The first two peaks are identical for both spectra and identified as the contribution of the two axial oxygen atoms and of five equatorial oxygen atoms. The third peaks, arising from the silicon contributions are at different positions for the two samples, while another peak appears for the sample prepared at pH 3. The corresponding results are summarized in the Table 3. The distance U–O_{axial} at 1.81 Å is the classical value for this ion. The equatorial contribution, which can be separated in two parts (3.0/2.7 $O_{equatorial}$ at 2.36 Å and 2.0/1.8 $O_{equatorial}$ at 2.54 Å), is due to two or three oxygen atoms belonging to the surface SiO_4 group and to two oxygen atoms belonging to hydroxyl groups or water hydration molecules. As the UO_2^{2+} in perchlorate solution ($C(U) = 10^{-3}$ M, $NaClO_4$ 0.5 M, pH = 3) is surrounded by five water molecules at 2.41 Å [40], the distance U–O_{axial} at 2.36 Å indicates clearly that uranyl ions have lost their water coordination sphere onto the $ZrSiO_4$ surface and consequently, they are linked to the surface oxygen atoms as an inner-sphere complex. The two different U–Si distances for both samples are not yet explained as well as the fourth peak that arises only on the sample prepared at pH = 3 and that could be due to the zirconium contribution. Moreover, in order to check whether the drying step, necessary for XPS measurement, could perturb the structure of the sorbed complex, in situ EXAFS experiments on wet samples have been performed. Both Fourier transforms for dried and wet samples are identical, which indicates that, in our experimental conditions, no change occurs during the drying step.

3.4. Determination of sorption constants

The retention data of the Cm^{3+}/bentonite system have been modeled using the structural information as experimental constraints. As this solid presents three types of functional sites (ion-exchange site, ≡S–Al–OH, ≡S–Si–OH), the bentonite acidity constants for the aluminol and silanol groups have been determined by simulation of the experimental titration curves of both alumina and silica using the CCM

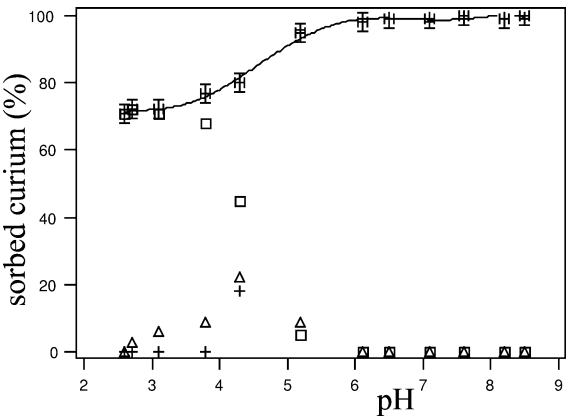

Figure 6. Cm/bentonite sorption curve (dots), corresponding simulation (line), □ exchange site, △=S–AlOH site, +=S–SiOH site.

model [41]. The equilibrium constant corresponding to the bentonite ion-exchange site has been determined by simulation of the sorption curve of cations (Na^+, Ca^{2+}, Mg^{2+}) on a purified sodic-montmorillonite [40]. The sorption curve (Fig. 6) has been obtained using 100 mg of bentonite in 10 mL of curium ($5 \cdot 10^{-8}$ M) solution (equilibrated with the clay). It corresponds to a concentration of $6.25 \cdot 10^{-4}$ M, $3.75 \cdot 10^{-5}$ M and $1.25 \cdot 10^{-3}$ M for the ion-exchange sites, aluminol and silanol sites, respectively. As the curium emission lifetime values have clearly indicated that the three functional sites interact with the curium ions depending on the pH of the solution, the simulation has been done taking into account these three sites. The silicate ions present in the suspension ($1.2 \cdot 10^{-4}$ M for the total concentration of H_4SiO_4) have been taken into account as well. The simulation of the experimental data has been performed using the CCM model (with a capacitance value of 1.2 F/m^2) and the following equilibria:

$$\begin{aligned}
\text{=S–AlOH}_2 &\Longleftrightarrow \text{=S–AlOH} + \text{H}^+, & \text{Log K} &= 7.90 \pm 0.03,\\
\text{=S–AlOH} &\Longleftrightarrow -\text{=S–AlO}^- + \text{H}^+, & \text{Log K} &= -9.22 \pm 0.05,\\
\text{=S–SiOH} &\Longleftrightarrow \text{=S–SiO}^- + \text{H}^+, & \text{Log K} &= -7.62 \pm 0.05,\\
\text{=X–Na} + \text{H}^+ &\Longleftrightarrow \text{=X–H} + \text{Na}^+, & \text{Log K} &= 1.0 \pm 0.05,\\
2\text{=X–Na} + \text{Ca}^{2+} &\Longleftrightarrow \text{=X}_2\text{–Ca} + 2\ \text{Na}^+, & \text{Log K} &= 2.7 \pm 0.05,\\
2\text{=X–Na} + \text{Mg}^{2+} &\Longleftrightarrow \text{=X}_2\text{–Mg} + 2\ \text{Na}^+, & \text{Log K} &= 2.4 \pm 0.05,\\
\text{=X–Na} + \text{K}^+ &\Longleftrightarrow \text{=X–K} + \text{Na}^+, & \text{Log K} &= 0.5 \pm 0.05,\\
\text{=X–Na} + \text{H}^+ + \text{H}_4\text{SiO}_4 &\Longleftrightarrow \text{=X–Si(OH)}_3 + \text{Na}^+ + \text{H}_2\text{O}, & \text{Log K} &= 6.0 \pm 0.5,\\
\text{=S–AlOH} + \text{H}_4\text{SiO}_4 &\Longleftrightarrow \text{=S–AlOSi(OH)}_3 + \text{H}_2\text{O}, & \text{Log K} &= 7.7 \pm 0.2.
\end{aligned}$$

The best fit of the experimental data, presented in Fig. 6 (experimental data and calculated curve), has been obtained considering the following equilibria that correspond to the structural results:

$$\begin{aligned}
\text{=S–(AlOH)}_2 + \text{Cm}^{3+} &\Longleftrightarrow \text{=S–(AlOH)}_2\text{Cm}^{3+}, & \text{Log K} &= 17.27 \pm 0.1,\\
\text{=S–(SiOH)}_2 + \text{H}_2\text{O} + \text{Cm}^{3+} &\Longleftrightarrow \text{=S–(SiO)}_2\text{Cm(OH)} + 3\ \text{H}^+, & \text{Log K} &= -9.64 \pm 0.8,\\
3\text{=X–Na} + \text{Cm}^{3+} &\Longleftrightarrow \text{=(X)}_3\text{–Cm} + 3\ \text{Na}^+, & \text{Log K} &= 5.33 \pm 0.02.
\end{aligned}$$

It is interesting to note that the calculated different individual site concentrations versus pH (Fig. 6) are in agreement with the structural investigation which indicates that at pH 3.1, the exchange site and the aluminol edge sites interact with the curium ions, while at pH 8.1, only the two silanol sites are occupied.

4. Conclusions

The examples, presented in this paper, have demonstrated the usefulness of an investigation at molecular level using spectroscopic techniques to investigate the sorption processes occurring at the solid/solution interface. The correlation of different spectrocopies has led to an unambiguous identification of the nature of the surface functional groups, the surface complexes loaded on the solids and the sorbed species structure. For instance, the uranyl ions are bounded to the oxygen atoms of the silicate groups of $ZrSiO_4$ surface as a polydendate inner-sphere complex whatever the background electrolyte ($NaClO_4$, KNO_3), while two species, the UO_2^{2+} ion and the nitrate complex $UO_2NO_3^+$ are present on the ZrO_2 surface in KNO_3 medium.

These structural results are then used to define the sorption equilibria that will be used to simulate the retention data. The trivalent curium, sorbed on the bentonite, presents four different decay times (depending on the pH value of the suspension) corresponding to the interlayer site and to aluminol and silanol edge sites. These structural results have been taken into account, as experimental constraints, in the simulation of the Cm/bentonite sorption curve, which allows the elimination of some mathematical solutions apparently acceptable.

At present, this methodology is well identified as a means to provide quantitative information on the sorption processes. Nevertheless, in order to improve the knowledge of the microscopic mechanisms, some studies on uranyl sorption on single crystal, such as ZrO_2 and TiO_2, have been started using GIXAS, XPS spectroscopies and ab initio quantum mechanical calculations [42].

Acknowledgements. I am very grateful to J. Lambert and J.J. Ehrhardt for the XPS measurements, J. Mielczarski for the DRIFT experiments and G. Lagarde for the optical experiments. Moreover, I am indebted to R. Drot, C. Lomenech, K. Ben Said and A. Kowal who are working on this topic since several years.

References

[1] C. Degueldre, H. Ulrich, H. Silby, Radiochim. Acta 65 (1994) 173.
[2] R. Guillaumont, Radiochim. Acta 66/67 (1994) 23.
[3] Ch. Papelis, K. Hayes, Colloids Surfaces A 107 (1996) 89.
[4] T.E. Payne, T.W. Waite, Radiochim. Acta 52/53 (1991) 487.
[5] S. Nagasak, S. Tanak, M. Todoriki, A. Suzuki, J. Alloys Compounds 271/273 (1998) 252.
[6] T.E. Payne, J.A. Davis, T.D. Waite, Radiochim. Acta 74 (1996) 239.
[7] C. Degueldre, B.J. Wernli, Environ. Radioactivity 20 (1993) 151.
[8] N.Z. Misa, Colloids Surface A 97 (1995) 129.
[9] K. Hayes, Ch. Papelis, J. Leckie, J. Colloid Interface Sci. 125 (1988) 717.
[10] N. Marmier, F. Fromage, J. Colloid Interface Sci. 212 (1999) 252.
[11] J.S. Noh, J.A. Schwarz, J. Colloid Interface Sci. 139 (1) (1990) 139–148.
[12] N. Marmier, A. Delisee, F. Fromage, J. Colloid Interface Sci. 211 (1) (1999) 54–60.
[13] R. Drot, C. Lindecker, B. Fourest, E. Simoni, New J. Chem. (1998) 1105–1109.
[14] A. Manceau, L. Charlet, J. Colloid Interface Sci. 168 (1994) 87.
[15] Y.D. Glinka, M. Jaroniec, V.M. Rozenbaum, J. Colloid Interface Sci. 194 (1997) 455.
[16] D. Morris, C. Chisholm-Brause, M. Bare, S. Conradson, P. Eller, Geochim. Cosmochim. Acta 58 (1994) 3613–3623.
[17] K.H. Chung, R. Klenze, K.K. Park, P. Paviet-Hartmann, I.J. Kim, Radiochim. Acta 82 (1998) 215–219.
[18] Th. Stumpf, Th. Rabung, R. Klenze, H. Geckeis, J.I. Kim, J. Colloid Interface Sci. 238 (2001) 219–224.
[19] C.M. Koretsky, D.S. Sverjensky, J.W. Salisbury, D.M. D'Aria, Geochim. Cosmochim. Acta 61 (11) (1997) 2193–2210.
[20] S.N. Towle, J.R. Bargar, G.E. Brown, G.A. Parks, J. Colloid Interface Sci. 217 (1999) 299–311.
[21] S.N. Towle, J.R. Bargar, G.E. Brown, G.A. Parks, J. Colloid Interface Sci. 217 (1999) 312–321.
[22] A.M. Scheidegger, G.M. Lamble, D.L. Sparks, J. Colloid Interface Sci. 186 (1997) 118–128.

[23] J. Shen, A.D. Ebner, A. Ritter, J. Colloid Interface Sci. 214 (1999) 333–343.
[24] S.I. Pechenyuk, Russ. Chem. Bull. 48 (1999) 1017–1023.
[25] T.W. Cheng, Minerals Engng. 13 (4) (2000) 105–109.
[26] A.V. Bekrenev, A.K. Pyartman, Inorg. Mater. 31 (11) (1995) 1315–1320.
[27] J.P. Reymond, F. Kolenda, Powder Technol. 103 (1999) 30–36.
[28] J.S. Noh, J.A. Schwarz, J. Colloid Sci. 139 (1) (1990) 139–148.
[29] J. Westall, H. Hohl, Adv. Colloid Interface Sci. 12 (1980) 265–294.
[30] A. Michalowicz, PhD thesis, Université du Val-de Marne, 1990.
[31] R. Mercier, M. Phan Thi, Ph. Colomban, Solid States Ionics 15 (1985) 113–126.
[32] A.L. Ankoudinov, J.J. Rehr, Phys. Rev. B 56 (1997) R1712.
[33] A.L. Ankudinov, Thesis, Washington University, 1996.
[34] H. Moll, G. Geipel, V. Brendler, G. Bernhard, H. Nitsche, J. Alloys Compounds 765 (1998) 271–273.
[35] W. De Horrocks Jr., D.R. Sudnick, J. Am. Chem. Soc. 101 (1979) 334.
[36] T. Kimura, G.R. Choppin, Z. Yoshida, Radiochim. Acta 72 (1996) 61–64.
[37] Y. Takahashi, T. Kimura, Y. Kato, Y. Minai, T. Tominaga, Radiochim. Acta 82 (1998) 227–232.
[38] I. Grenthe, Chemical Thermodynamical of Uranium, Elsevier, Amsterdam, 1992.
[39] V. Eliet, PhD thesis, Université de Paris XI, 1996.
[40] R. Drot, E. Simoni, Ch. Denauwer, C. R. Acad. Sci. Paris Sér. IIc 2 (1999) 111–117.
[41] N. Marmier, private communication.
[42] C. Domain, H. Catalette, private communication.

Discussion

Commentaire de P. Toulhoat

Les exemples cités illustrent le comportement de l'UO_2^{2+}, forme oxydée de l'uranium en solution. En stockage profond, l'uranium sera réduit (U^{4+}). Par contre, en cas de perturbation oxydante, on constate que l'adsorption est très efficace pour immobiliser l'uranium.

Question de É. Brézin

Y a-t-il des liens entre ces études de sorption et les propriétés de mouillage des surfaces ? Quelles sont les implications pour ces questions de migrations ?

Réponse de E. Simoni

On peut difficilement parler de mouillage avec des échantillons sous forme de poudre poly cristalline. En fait, l'eau au contact de la surface se dissocie et hydroxyle les groupements de surface.

Question de G. de Marsily

Prenez-vous en compte dans le modèle que vous avez présenté les interactions coulombiennes ?

Réponse de E. Simoni

Oui. Cette interaction coulombienne est prise en compte dans un terme exponentiel dans la constante thermodynamique de sorption.